Carbohydrate Polymers 181 (2018) 633–641

Contents lists available at ScienceDirect

Carbohydrate Polymers

journal homepage: www.elsevier.com/locate/carbpol

Reactivity of main components and substituent distribution in esterified sugarcane bagasse prepared by effective solid phase reaction

Tao Gan[a], Yanjuan Zhang[a,*], Yane Chen[a], Huayu Hu[a], Mei Yang[a], Zuqiang Huang[a,*], Dong Chen[b], Aimin Huang[a]

[a] School of Chemistry and Chemical Engineering, Guangxi University, Nanning, 530004, China
[b] State Key Laboratory of Non-Food Biomass and Enzyme Technology, Guangxi Academy of Sciences, Nanning, 530007, China

ARTICLE INFO

Keywords:
Lignocellulose
Cellulose
Esterification
Mechanical activation
Solid phase reaction
Reactivity

ABSTRACT

Three main components of lignocellulose (cellulose, hemicellulose, and lignin isolated from sugarcane bagasse (SCB)) as well as holocellulose and SCB were modified with maleic acid by mechanical activation (MA)-assisted solid phase reaction (MASPR) technology. The order of reactivity was found to be lignin > hemicellulose > cellulose. The amorphous structure of lignin and hemicellulose mainly attributed to their better reactivity, and the modified lignin could reach a maximum degree of esterification (DE) of 93.45%. MA improved the accessibility and reactivity of cellulose, as the DE of modified cellulose gradually increased with milling time and reached the maximum value of 57.30% at 120 min, which had significant effect on structure changes and DE of modified holocellulose and SCB. MA enhanced the esterification of all three components in lignocellulose with relatively high substituent distribution in them, and maleated SCB with a maximum DE of 64.17% was successfully prepared by this simple, green, and effective MASPR technology.

1. Introduction

Sugarcane, a main sugar crop, is widely cultivated in tropical and subtropical regions. Sugarcane bagasse (SCB) is the fibrous residue of cane stalks left over after the crushing and extraction of the juice from sugarcane (Pandey, Soccol, Nigam, & Soccol, 2000). Therefore, SCB is an abundant, inexpensive and readily available source of lignocellulosic biomass (Zhang & Wu, 2014), which can be considered as an almost inexhaustible source of raw material for the preparation of environmentally friendly and biocompatible products (Leibbrandt, Knoetze, & Görgens, 2011; Nakasone, Ikematsu, & Kobayashi, 2016; Sakdaronnarong et al., 2016). In order to improve the properties of lignocellulose, including dimensional stability, resistance to fungal attack, and mechanical properties, chemical modification with dicarboxylic acids or anhydrides is an effective and promising approach to satisfy the above mentioned demands (Doczekalska, Bartkowiak, & Zakrzewski, 2014; Hundhausen, Kloeser, & Mai, 2015; Iwamoto & Itoh, 2005; Vaidya et al., 2016).

Lignocellulose mainly consists of cellulose (~50%), hemicellulose (~25%), and lignin (~25%), which associate with each other to form a supermolecular structure by hydrogen bonds and some other covalent bonds. Cellulose is a linear natural polymer of anhydroglucose units linked by β-1,4-glycosidic bonds. The three hydroxyl groups with different acidity/reactivity in anhydroglucose units form strong inter- and intramolecular hydrogen bonds, leading to the formation of highly-ordered and stable crystal structure of cellulose (Sun, Sun, Zhao, & Sun, 2004). Hemicellulose, branches with short lateral chains that usually composed of easy hydrolyzable polymers (including xylose, arabinose, galactose, glucose, and mannose), is an amorphous polymer and has a lower molecular weight than cellulose (Hendriks & Zeeman, 2009; Ren et al., 2007). Lignin is composed of three phenyl propane units called *p*-hydroxyl phenyl propane (H), guaiacyl (G), and syringyl (S) units, which are connected in a disorderly manner with C—C and C—O bonds and form a three-dimensional network. Lignin also contains a lot of functional groups, such as aliphatic hydroxyls, phenolic hydroxyls, carboxyls, carbonyls, and methoxyls (Kai et al., 2016). Lignocellulose can be chemically modified by the substitution reactions of the hydroxyl groups in cellulose, hemicelluloses, and lignin. However, these three main components in lignocellulose have characteristic chemical and crystal structures, contributing to different reactivity of their hydroxyl groups.

Generally, chemical modification of cellulosic materials is performed in organic solvents in either heterogeneous or homogeneous reaction system (Boufi & Belgacem, 2006; Chen, Chen, Liu, & Sun, 2013; Crépy, Miri, Joly, Martin, & Lefebvre, 2011; Freire et al., 2008). In these reactions, it is necessary to separate and properly dispose or

* Corresponding authors.
E-mail addresses: zhangyj@gxu.edu.cn (Y. Zhang), huangzq@gxu.edu.cn (Z. Huang).

https://doi.org/10.1016/j.carbpol.2017.11.102
Received 6 September 2017; Received in revised form 1 November 2017; Accepted 27 November 2017
Available online 29 November 2017
0144-8617/ © 2017 Elsevier Ltd. All rights reserved.

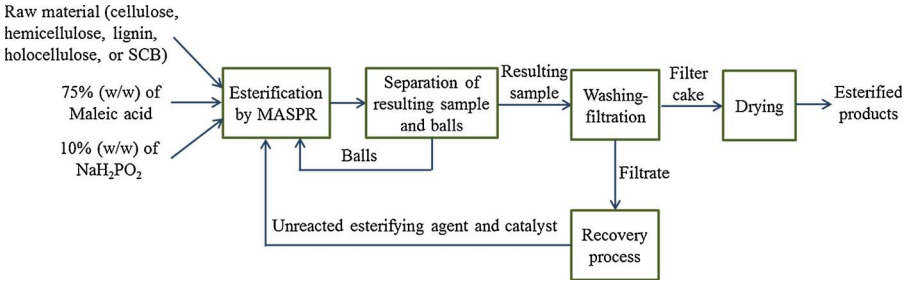

Fig. 1. Flow diagram of the esterification of different samples by MASPR.

recycle the used organic solvents due to toxic, corrosive nature and unpleasant odour of the effluents. In addition, the products need extraction and purification steps. These treatments decrease the economic feasibility of the whole process (Vaidya et al., 2016). Recent years, solid phase reaction (SPR) has been attracting more and more attentions for the advantages of nonuse of organic solvent, high selectivity and efficiency, and simple operation of reaction and purification processes. However, mass transfer and heat transfer in SPR system are very poor, especially the reactants with stable and compact structure. Therefore, SPR is difficult to carry out under common reaction conditions, and assisted means is necessary to improve the contacting state between reactants and promote the reactivity of the solid materials with stable and recalcitrant structure. In our laboratory, we have applied mechanical activation (MA) to enhance the chemical modification of natural polymers by SPR, and this technology is defined as MA-assisted SPR (MASPR) (Zhang, Gan, Hu et al., 2014; Zhang, Gan, Luo et al., 2014). For the chemical modification of cellulosic materials by MASPR, the general problem is to accomplish as a sufficient penetration of the chemical agents into cellulosic materials. Cellulose, hemicelluloses, and lignin possess their special chemical and crystal structures, so it is interesting and significant to investigate the reaction characteristics of these three main components in lignocellulose.

For these reasons, the present work was to comparatively study the reactivity of monocomponents and multicomponents in SCB, including cellulose, hemicellulose, lignin, holocellulose (cellulose + hemicellulose), and lignocellulose (SCB itself), with maleic acid as esterifying agent by MASPR. Moreover, in order to comprehensively study the strengthening mechanism of MA for enhancing the reactivity of cellulosic materials during the process of MASPR, these materials were also treated by MA without any chemical reagent to accurately measure the structure changes induced by MA. The degree of esterification (DE) of different components was determined by measuring the content of carboxylic groups (C_{COOH}), and Fourier transform infrared spectroscopy (FTIR), solid state CP/MAS ^{13}C NMR, X-ray diffractometry (XRD), and scanning electron microscopy (SEM) were applied to measure the changes in chemical, crystal, and morphological structures after MA treatment and MASPR modification. It is expected that these data can efficiently analyze the reactivity of different components in lignocellulose and understand the substituent distribution in esterified lignocellulose prepared by MASPR.

2. Materials and methods

2.1. Materials

SCB was used as lignocellulose material and was obtained from a local sugar factory (Nanning, China), which was sieved through a standard sieve of 60 mesh size (250 μm). It contained 44.04% cellulose, 30.77% hemicellulose, 22.80% lignin, and 2.39% ash and others. All chemical reagents were obtained commercially and were analytical grade without further purification.

2.2. Isolation of different components from SCB

Cellulose, hemicellulose, lignin, and holocellulose were isolated from SCB. Cellulose, hemicellulose, and holocellulose were prepared according to the reported procedure (Rowell et al., 1994; Vaidya et al., 2014). Lignin was prepared following the method of Xiao, Sun, & Sun (2001). All these samples were dried in an oven at 105 °C for 12 h before use.

2.3. Esterification of different samples by MASPR

Esterification of cellulose, hemicellulose, lignin, holocellulose, and SCB was performed by MASPR procedure in a customized stirring ball mill (Zhao et al., 2016). A fixed amount of milling balls (300 mL, 5 mm diameter) was first put in a jacketed stainless steel tank (1200 mL). Then, dry sample (10 g) was mixed with 75% w/w esterifying agent (maleic acid) and 10% w/w catalyst (sodium hypophosphite). The mixture was put into the tank and was subjected to dry milling at a fixed stirring speed of 300 rpm, and the reaction temperature was fixed at 80 °C by circulating the thermostatic water in the jacket of tank. When the mixture was milled for desired reaction time (milling time), the balls were removed from the resulting sample by a sieve. The crude product was purified by a repeated washing-filtration process with deionized water (maleated hemicellulose was washed by alcohol) until the filtrate was neutral to remove unreacted reagents, and the filtrate was collected for analysis by high performance liquid chromatography (HPLC, LC-6AD, SHIMADZU, Japan). The filter cake was vacuum-dried at 55 °C for 48 h, and then the resulting product was obtained. The flow diagram of the esterification of different samples by MASPR is illustrated in Fig. 1.

2.4. MA treatment

MA treatment of the samples was operated in the same way as in MASPR, except for the non-addition of chemical reagents (maleic acid, sodium hypophosphite). The resulting sample was oven-dried at 55 °C for 12 h and then sealed for characterization.

2.5. Determination of DE

DE of the chemical modified samples was calculated by measuring the C_{COOH} in them, and DE value was the ratio of the measured C_{COOH} value to the theoretical maximum C_{COOH} value. The C_{COOH} of modified cellulose, hemicellulose, holocellulose, and SCB was measured by the acid-base titration method as follows (Gurgel, Júnior, Gil, & Gil, 2008): 0.1 g of the sample was precisely weighed and was mixed with 100 mL of 0.01 mol L^{-1} NaOH solution in a 250 mL conical flask. The solution was stirred at a constant temperature of 30 °C for 1 h, and then was filtered. Finally, 25 mL of filtrate was titrated with 0.01 mol L^{-1} standard HCl solution. The C_{COOH} of modified lignin was measured by the potentiometric titration method as follows (Gosselink et al., 2004): 1.0 g of the sample was accurately weighed and then was added in 10 mL NaOH solution. After stirred for 1 h, the pH was adjusted to 12 with NaOH solution. After another 2 h stirring, the solution was

potentiometrically titrated with 0.1 mol L^{-1} standard HCl solution.

2.6. Characterization

FTIR spectra were recorded on a FTIR-8400S Spectrometer (SHIMADZU, Japan) at a resolution of 4 cm^{-1} in a frequency range from 400 to 4000 cm^{-1}. XRD measurement was carried out on a D/MAX2500 V diffractometer (Rigaku, Japan) using Cu K_α radiation (λ = 0.154 nm) at 40 kV and 30 mA, with a step size of 0.02° and a recorded range from 5° to 50°. SEM observation was operated using an S-3400N scanning electron microscope (Hitachi, Japan) at an accelerating voltage of 5 kV and a working distance of 6.5 mm, and the samples were fixed on a sample holder using double-sided tape and coated with a thin layer of gold to improve the conductivity. Solid state CP/MAS (cross-polarisation, magic angle spinning) ^{13}C NMR spectra of the samples were accumulated on an AVANCE AV 400 (Bruker, Germany) operating at ^{13}C 100.62 MHz. Each 90° proton preparation pulse of 2.1 μs was followed by a cross polarisation time of 1.0 ms, contact time of 1.5 s, and a pulse delay of 2.0 s. All chemical shifts were reported in parts per million (ppm).

3. Results and discussion

3.1. Comparison of the chemical reactivity of different components in SCB

All of the three components of lignocellulose are rich in hydroxyl groups, which can react with other reagents to modify their performances. For this purpose, it is significant to evaluate the active and recalcitrant components in lignocellulose under a certain reaction condition. Herein, the chemical reactivity of different components of SCB in MASPR system was determined by comparing the C_{COOH} and DE values, and the results are presented in Fig. 2.

For lignin isolated from SCB, a C_{COOH} value of 2.155 mmol g^{-1} was obtained at the reaction time of 30 min and a maximum C_{COOH} value of 3.712 mmol g^{-1} was achieved at the reaction time of 90 min. Lignin is confirmed to be composed of three phenyl propane monolignols units which are polymerized via radical coupling reactions to form a complex three-dimensional molecular architecture that contains a great variety of bonds (Laurichesse & Avérous, 2014; Upton & Kasko, 2016), and the theoretical maximum C_{COOH} of maleated lignin is 3.961 mmol g^{-1}, for 1.2 hydroxyl groups per C_9 unit (Kirk, 1975). The maximum DE of modified lignin could reach 93.45%, evidently indicating that lignin was the most reactive component in SCB. For hemicellulose isolated from SCB, the C_{COOH} of maleated hemicellulose rapidly reached 1.917 mmol g^{-1} at the reaction time of 30 min, but it almost did not increase as prolonging the reaction time. As an increment of reaction time to 90 min, the C_{COOH} slowly increased to the maximum value of 2.291 mmol g^{-1}. Hemicellulose is heteropolysaccharides in the plant cell wall, and xylose was the predominant sugar component. While mannose and glucose were small amounts, and rhamnose, arabinose, and galactose were minor sugar constituents (Sun, Fang, Tomkinson, Geng, & Liu, 2001; Sun, Sun, Sun, & Su, 2004). Therefore, hemicellulose is mainly consisted of pentose sugar units for 2 hydroxyl groups per C_5 unit, and the theoretical maximum C_{COOH} of maleated hemicellulose is 6.097 mmol g^{-1}. Although the maximum DE of modified hemicellulose was only 37.57% at 90 min, it is the second reactive component in SCB as the DE quickly reached a higher value of 31.45% at initial 30 min. To analyze why the reactivity of hemicellulose decreased as increasing the reaction time, the filtrate collected from washing purification process of maleated hemicellulose was measured by HPLC, and a large number of oligosaccharides and monosaccharides were detected, showing that the stability of single hemicellulose component was poor and the polysaccharides backbones were easily decomposed, especially under intense mechanical milling. As a result, the chemical modification of hemicellulose was difficult to go smoothly. Cellulose is considered as a recalcitrant component in lignocellulose, and it hardly react with chemical reagents without activation pretreatment because of its highly-ordered and stable crystalline structure ascribed to strong inter- and intramolecular hydrogen bonds. Rowell et al. (1994) reported that the reactivity of cellulose isolated from pine was almost zero as reacted with acetic anhydride, mainly ascribing to low accessibility of hydroxyl groups in cellulose. Undoubtedly, esterification of cellulose is impossible took place under common solid state reaction conditions. For the esterification of cellulose by MASPR, intense milling could effectively destroy its recalcitrant structure and enhance the contact between esterifying agents and the hydroxyl groups of cellulose. Obviously, the C_{COOH} of maleated cellulose gradually increased with increasing the milling time, from 1.386 mmol g^{-1} (30 min) to 3.770 mmol g^{-1} (120 min). Cellulose is polydisperse linear polymer of β-1,4-D-glucose for 3 hydroxyl groups per C_6 unit (Yang, Zhang, & Xu, 2015), and the theoretical maximum C_{COOH} of maleated cellulose is 6.579 mmol g^{-1}. Therefore, the maximum DE of modified cellulose could reach 57.30%, due to the improved reactivity of cellulose by MA.

In order to further investigate the reactivity of different components of SCB, multicomponents (holocellulose and lignocellulose) were also esterified by MASPR. Holocellulose, prepared from SCB by the removal of lignin, is a combined component consisted of cellulose and hemicellulose, and the theoretical maximum C_{COOH} of maleated holocellulose is 6.381 mmol g^{-1}. Normally, the C_{COOH} of maleated holocellulose should equal to the sum of those of maleated cellulose and hemicellulose. It seems that the esterification of holocellulose approximately reflected the combined results of esterified cellulose and hemicellulose. Nevertheless, these two components were cross-linked with each other, and the structure of holocellulose was more stable than that of single component. At the initial reaction stage, the DE of maleated holocellulose was lower than both of maleated cellulose and hemicellulose, ascribing to that the stable structure of holocellulose was not effectively destroyed by less milling time. As sequentially increasing the milling time, the DE of maleated holocellulose gradually increased, which exceeded the sum of those of maleated cellulose and hemicellulose, implying that cross-linked structure could protect hemicellulose from hydrolysis and thus improved the esterification of holocellulose. After 120 min of esterification, the C_{COOH} and DE of maleated holocellulose could reach 3.193 mmol g^{-1} and 50.04%, respectively. SCB

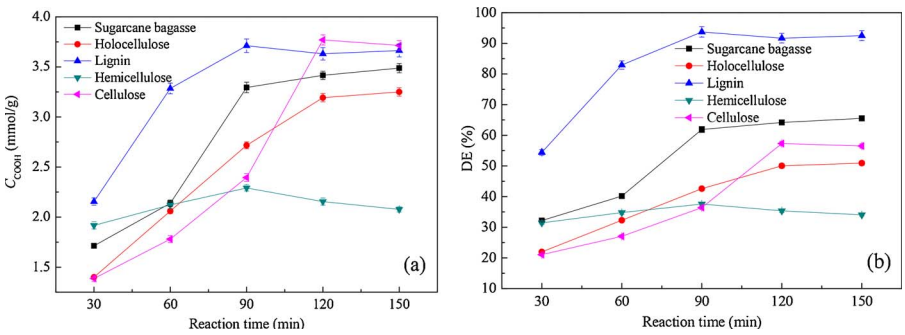

Fig. 2. Effect of reaction time on C_{COOH} and DE values of different modified samples.

represented the whole structure of lignocellulose, and the esterification of SCB revealed the comprehensive results of esterified lignin, hemicellulose, and cellulose. These three monocomponents in SCB associate with each other to form a highly-ordered cellulose-hemicellulose-lignin supermolecular structure by hydrogen bonds and some other covalent bonds, so the esterification of SCB was not a simple superposition of that of three components. Not only the reactivity of each component but also the native structure of lignocellulose affected the esterification of SCB. After 120 min of esterification, the C_{COOH} and DE of maleated SCB could reach 3.416 mmol g^{-1} and 64.17%, respectively. Consequently, the order of reactivity was determined to be lignin > hemicellulose > cellulose, indicating that increasing the reactivity of cellulose was the main critical process to enhance the chemical modification of lignocellulose. The assistance of MA significantly improved the reactivity of every component of SCB in solid phase reaction system without the use of solvents, and the unreacted esterifying agent and catalyst could be recycled by water or ethanol washing and the corresponding recovery processes. Therefore, modification of lignocellulosic biomass by MASPR technology can effectively prevent loss of materials and pollution to environment, and it would be particularly beneficial for industrialization.

3.2. Chemical structure by FTIR analysis

The titrimetric results were confirmed by FTIR analysis, which could also further examine the functional groups and chemical structure of the samples before and after MA treatment and MASPR modification. FTIR spectra of original, MA treated, and MASPR modified samples are illustrated in Fig. 3.

As shown in Fig. 3a, the spectrum of original lignin shows characteristic peaks at 1598, 1511, 1460, and 1422 cm^{-1}, corresponding to aromatic skeleton vibrations (Zhou, Chang, Wu, Yang, & Qiu, 2015), which confirmed that this isolated component was lignin. Lignin contains phenolic hydroxyls with higher reactivity (Zhao et al., 2017), contributing to that lignin was easier to react with esterifying agent than hemicellulose and cellulose, which only contain aliphatic hydroxyls. After 120 min of MA treatment, a peak at 1698 cm^{-1} corresponding to carbonyl group became stronger, which may be due to the oxidation of phenolic hydroxyl groups and the generation of aldehyde, ketone, or carboxyl groups. In addition, an absorption peak of stretching vibration of aromatic and aliphatic −OH groups shifted from 3421 cm^{-1} to a higher wavenumber of 3436 cm^{-1}, indicating that MA increased the hydrogen bond energy and thus enhanced the reactivity of lignin. Obviously, the spectrum of MASPR modified lignin shows a new peak at 1717 cm^{-1}, which was the overlapping characteristic absorption peaks of carboxyl and ester carbonyl groups, confirming the successful esterification of lignin.

FTIR spectra of different hemicellulose samples are presented in Fig. 3b. In the spectrum of original hemicellulose, the characteristic signature frequencies of hemicellulose are shown at 3426, 2917, 1375, and 1044 cm^{-1} (Vaidya et al., 2016), corresponding to O−H stretching vibration, C−H stretching vibration, C−H bending, and C−O ether vibration of xylopyranose, respectively. The peak at 896 cm^{-1} is assigned to C−H out-of-plane in position ring stretching originated from β-glucosidic linkages between the sugar units, corroborating that the xylose residues forming the backbone of the macromolecule are linked by β-form bonds (Xu et al., 2008). After MA treatment, the peak of O−H stretching vibration (hydroxyl groups) shifted from 3422 to 3432 cm^{-1}, indicating the increase of internal energy and reactivity of hemicellulose induced by MA. Esterification of hemicellulose was confirmed by the new peaks at 1730, 1583, and 823 cm^{-1}, attributed to stretching vibration of carbonyl in ester groups, C=O stretching of carboxyl groups, and =C−H stretching in maleate groups, respectively.

Fig. 3c presents the spectra of different cellulose samples. Fig. 3c-1 shows the characteristic peaks of original cellulose at 3417, 2896, 1430, 1380, 1261, 1167, and 1057 cm^{-1}, corresponding to stretching vibration of −OH groups, C−H stretching vibration, CH_2 bending, C−H bending, OH in-plane bending of cellulose, C−O antisymmetric bridge stretching, and C−O−C pyranose ring skeletal vibration, respectively (Sun, Xu, Sun, Xiao, & Sun, 2005). No new absorption peak appearing in the spectrum of MA-treated sample indicates that MA did not change the chemical structure of cellulose, but MA could increase the internal energy of cellulose and weaken the stability of hydrogen bond as the peak of O−H stretching vibration shifted from 3417 to 3427 cm^{-1}. The difficulty of native cellulose to contact and react with chemical reagents was mainly ascribed to its stable hydrogen bonds and highly-ordered crystal structure, so MA could effectively enhance its accessibility and reactivity. With the assistance of MA in SPR system, maleated cellulose was successful produced, which was proved by the peaks at 1731 and 823 cm^{-1} attributed to the characteristics of carbonyl in ester groups and =C−H in maleated groups, respectively. Evidently, FTIR analysis confirmed that all these three monocomponents had been successfully esterified by MASPR.

Furthermore, the same method was also used to measure the chemical structure of holocellulose and SCB, and the results are illustrated in Fig. 3d and e, respectively. FTIR spectra of holocellulose show the characteristic adsorption peaks of cellulose and hemicellulose, and that of SCB shows the characteristic adsorption peaks of cellulose, lignin, and hemicellulose. There was a little difference between spectrum of holocellulose and that of hemicellulose: a peak at 1735 cm^{-1}, attributed to the acetyl, uronic, and ferulic ester groups of the polysaccharides in hemicellulose (Sun, Sun, Sun et al., 2004; Sun, Sun, Zhao et al., 2004), was shown in the spectrum of holocellulose but was not shown in that of hemicellulose. This phenomenon may be due to that these water-soluble polysaccharides was easily hydrolyzed and was not collected while isolated the hemicellulose monocomponent, but hemicellulose combined with cellulose could inhibit the hydrolysis of these polysaccharides, so they could present in holocellulose. Effect of MA treatment on holocellulose and SCB was the same as on three monocomponents for the increase of internal energy and enhancement of reactivity. Undoubtedly, holocellulose and SCB were esterified by MASPR as new peaks generated at around 1730 and 823 cm^{-1}, corresponding to stretching vibration of carbonyl in ester groups and =C−H stretching in maleate groups, respectively.

3.3. Chemical structure by solid state CP/MAS ^{13}C NMR analysis

Solid state CP/MAS ^{13}C NMR is the most effective of the few methods for the characterization of lignocellulosic materials, as it can directly provide detailed information on solid samples to further validate the FTIR results (Liu et al., 2007; Love et al., 1998). The changes in chemical structure of lignin, hemicellulose, cellulose, holocellulose, and SCB before and after MA treatment and MASPR modification were investigated by solid state CP/MAS ^{13}C NMR, and the spectra are presented in Fig. 4.

For the spectrum of original lignin shown in Fig. 4a-1, the peaks at 100–155 and 20–90 ppm correspond to the signals from aromatic carbon and aliphatic carbon, respectively (Fox & McDonald, 2010). The characteristic signals at 165–180 and 33.7 ppm correspond to carbonyl units and methylene bridges between aromatic nuclei, respectively. The intensity of these two signals increased after MA treatment, indicating that the oxidation of lignin by demethylation and depolymerization/repolymerization could be induced by MA (Zhao et al., 2016). In the spectrum of MASPR modified lignin, intensity of the signals at 165–180 and 135.2 ppm assigned to C=O and C=C increased, indicating that maleic acid had been grafted onto lignin.

Fig. 4b shows the CP/MAS ^{13}C NMR spectra of original as well as MA treated and MASPR modified hemicellulose samples. The main 1,4-linked β-D-Xylp units in hemicellulose were obviously confirmed by strong signals at 105.7, 70.0–85.0, and 64.4 ppm, which are assigned to C-1, C-4,3,2, and C-5 positions of the β-D-Xylp units, respectively (Beramendi-Orosco, Castro-Diaz, Snape, Vane, & Large, 2004; Sun, Sun,

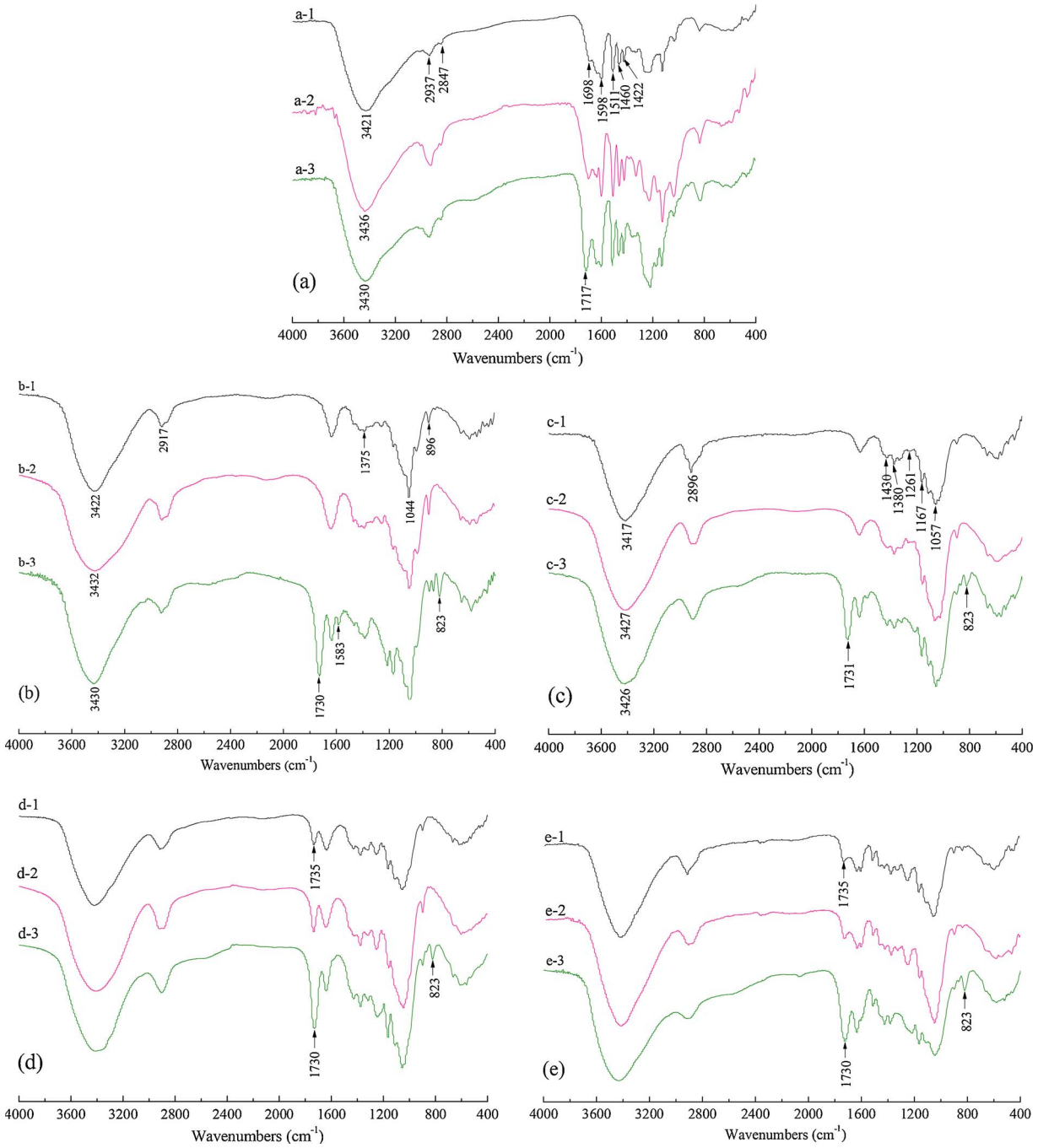

Fig. 3. FTIR spectra of different samples: (a) lignin, (b) hemicellulose, (c) cellulose, (d) holocellulose, (e) SCB, and 1, 2, 3 represent original, MA treated (120 min), MASPR modified (120 min), respectively.

Sun et al., 2004; Sun, Sun, Zhao et al., 2004). There was not any change in the spectrum of MA treated hemicellulose, implying that MA did not affect the structure of hemicellulose. In the spectrum of modified hemicellulose, the signals appeared at 169.2 and 136.8 ppm corresponding to C═O and C═C carbon atoms in maleate groups, respectively, demonstrating the esterification of hemicellulose with maleic acid by MASPR. Moreover, a distinguishing peak appeared at 83.4 ppm indicated that the hydroxyl groups in C-3,2 position had reacted with esterifying agent.

CP/MAS ^{13}C NMR analysis of different cellulose samples are presented in Fig. 4c. For the spectrum of original cellulose, all major signals of the carbon atoms of carbohydrate moiety are distributed in the region between 55 and 110 ppm. The signals at 105.6, 89.5, 83.3, 75.5, 73.4, 65.9, and 63.5 ppm are assigned to C-1, C-4 of crystalline cellulose, C-4 of amorphous cellulose, C-2,3, C-5, C-6 of crystalline cellulose, and C-6 of amorphous cellulose, respectively (Tang et al., 2013; Vaidya et al., 2016). The spectrum of MA treated cellulose obviously changed as the disappearance of 89.5 and 65.9 ppm for crystalline cellulose and the broadening of 83.3 and 63.5 ppm for amorphous cellulose, indicating that MA destroyed the crystal structure and the amorphous region increased, which helped to improve the accessibility and reactivity of cellulose. Although cellulose possesses the lowest reactivity in lignocellulose, the strengthening effect of MA was effective to enhance the esterification of cellulose, and the dependency of cellulose on MA was stronger than that of lignin and hemicellulose. As presented in Fig. 4c-3, the spectrum of MASPR modified cellulose showed new signals at 167.3 and 137.7 ppm attributed to the presence of C═O and C═C carbon atoms in maleate groups, respectively,

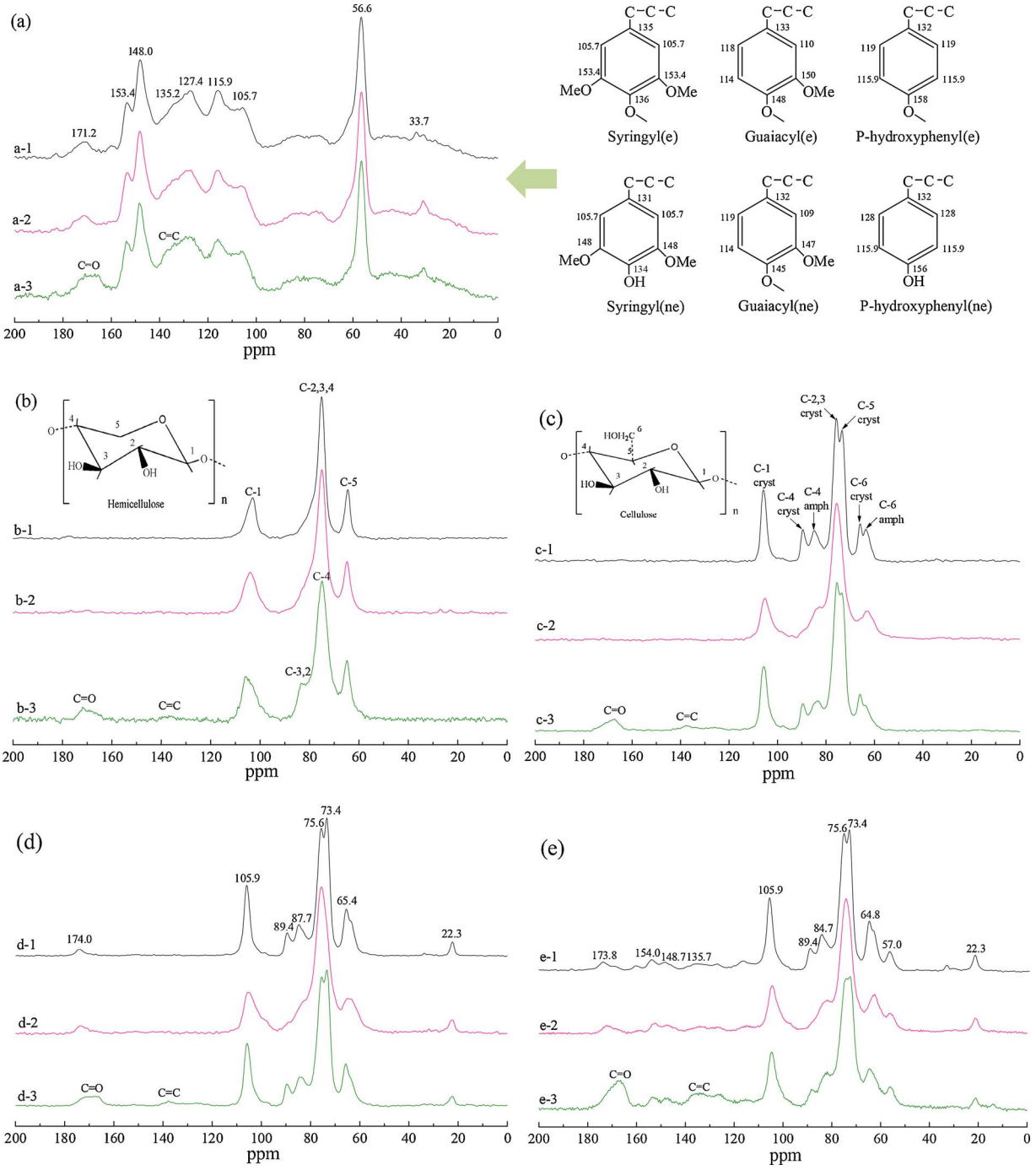

Fig. 4. CP/MAS ^{13}C NMR spectra of different samples: (a) lignin, (b) hemicellulose, (c) cellulose, (d) holocellulose, (e) SCB, and 1, 2, 3 represent original, MA treated (120 min), MASPR modified (120 min), respectively.

confirming the maleylation of cellulose.

CP/MAS ^{13}C NMR analysis of different holocellulose and SCB samples were also carried out and the results are presented in Fig. 4d and e. ^{13}C NMR spectrum of holocellulose showed all the signals in the monocomponents of cellulose and hemicellulose. In addition, the signals at 174.0 and 22.3 ppm attributed to the acetyl, uronic, and ferulic ester groups of the polysaccharides and inherent acetylation of native hemicellulose appeared in the spectrum of holocellulose but do not in that of hemicellulose, indicating the easy hydrolysis of these constituents, which is well consistent with FTIR result. Similarly, the spectrum of SCB presented the total signals of cellulose, lignin, and hemicellulose. MA treatment could destroy the crystal structure of both holocellulose and SCB, and thus enhanced their reactivity. The increase in intensity of the signals at 173.8 and 135.7 ppm assigned to C═O and C═C in the spectra of modified samples confirmed the maleylation of holocellulose and SCB by MASPR.

3.4. Morphology observation by SEM analysis

The morphological changes in the samples before and after MA treatment and MASPR modification are shown in Fig. 5. The surface of original lignin and hemicellulose was rough and porous, coated with many irregular particles, confirming their better accessibility and reactivity. After MA treatment and MASPR modification, the surface structure of lignin and hemicellulose was not obviously changed, mainly the changes in distribution of porosity. Different from lignin and

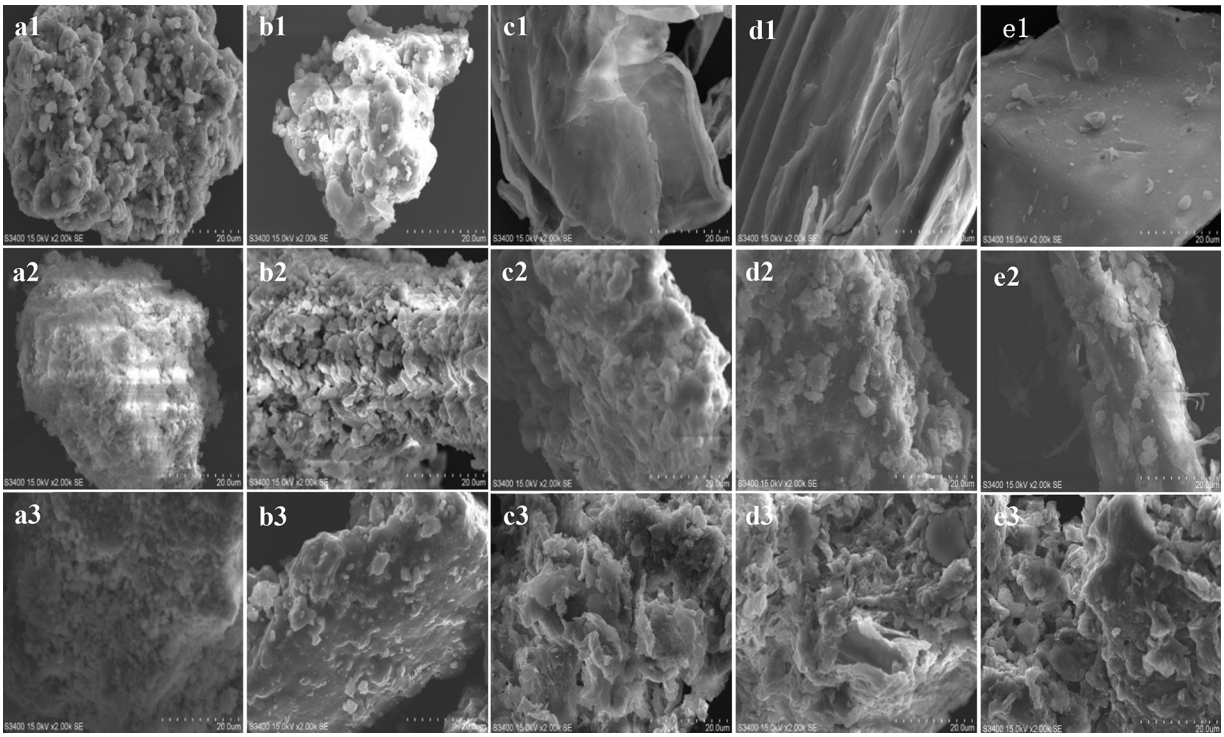

Fig. 5. SEM micrographs of different samples: (a) lignin, (b) hemicellulose, (c) cellulose, (d) holocellulose, (e) SCB, and 1, 2, 3 represent original, MA treated (120 min), MASPR modified (120 min), respectively.

hemicellulose, the original cellulose, holocellulose, and SCB consist of fiber bundles with compact and smooth surfaces. After MA treatment and MASPR modification, these three samples were greatly destroyed and the fiber bundles were split and fractured to produce small particles with irregular and rough surfaces. For the destruction of compact structure and increase of amorphous structure and specific surface area, the reagents could easily contact and react with the hydroxyl groups, which thus increased the accessibility and reactivity of cellulose, holocellulose, and SCB. Consequently, the destruction of the stable structure of crystalline materials by MA played an important role for enhancing the chemical modification in solid phase reaction system.

3.5. Crystal structure by XRD analysis

For crystalline solid materials, XRD analysis is a reliable indicator for measuring the transformation of its structure. As lignin and hemicellulose are mainly amorphous polymers in plant biomass (Ren et al., 2007; Tran et al., 2016), only three crystalline samples (cellulose, holocellulose, and SCB) were characterized by XRD analysis, and the results are presented in Fig. 6.

The crystalline region in holocellulose and SCB is mainly attributed to the containing of cellulose, so XRD patterns of all these three samples are similar. The four characteristic peaks at 2θ = 15.1°, 16.2°, 22.2°, and 34.7° corresponded to 101, 10-1, 002, and 040 diffraction planes of the cellulose I crystalline form, respectively (Liao, Huang, Hu, Zhang, & Tan, 2011). The intensity of diffraction peaks of MA treated samples was weaker than that of original ones, and the diffraction peaks became broadening. These reveal that MA significantly destroyed the stable hydrogen bonds in these samples and caused the fracture of macromolecular chains, the destruction of crystalline structure, the variation of crystallite size, and the increase of amorphous region (Zhang, Gan, Luo et al., 2014), which agree well with the results of above analyses. Compared with the patterns of MA treated samples, the diffraction intensities of MASPR modified samples were stronger, resulting from the weakening of direct mechanical milling on the crystalline materials in the presence of esterifying agent and catalysis and new crystallization of grafted side chains. Evidently, the breaking of crystal structure of cellulose by MA provided significant effect on improving the reactivity of cellulose, holocellulose, and SCB.

4. Conclusions

The comparative investigation for chemical modification of the main components isolated from SCB by MASPR showed that the order of reactivity was lignin > hemicellulose > cellulose. The highest reactivity of lignin mainly attributed to the containing of phenolic hydroxyls and its amorphous structure. The maleylation of lignin and hemicellulose rapidly reached high DE in initial reaction stage, and the maximum DE values were obtained to be 94.45% and 37.57% at 90 min. Modified hemicellulose did not gain a higher DE as increasing the reaction time due to that the stability of single hemicellulose component was poor and the polysaccharides backbones were easily decomposed. Cellulose is a recalcitrant component in lignocellulose with poor reactivity because of its stable crystalline structure. MA could effectively destroy the inter- and intramolecular hydrogen bonds, compact fibrous structure, and crystalline structure of cellulose and thus improved its accessibility and reactivity, as the DE of modified cellulose gradually increased with milling time and reached the maximum value of 57.30% at 120 min. As the most important component of lignocellulose, the structure changes and esterification of cellulose had significant effect on those of holocellulose and SCB. MA enhanced the esterification of all three components in lignocellulose with relatively high substituent distribution in them, and maleated SCB with a maximum DE of 64.17% was successfully produced by MASPR technology. MASPR could be considered as a simple, environmentally friendly, and effective method for chemical modification of lignocellulose.

Acknowledgements

This research was supported by National Natural Science Foundation of China (No. 51463003 and 21666005), Guangxi Natural Science Foundation of China (No. 2017GXNSFEA198001 and

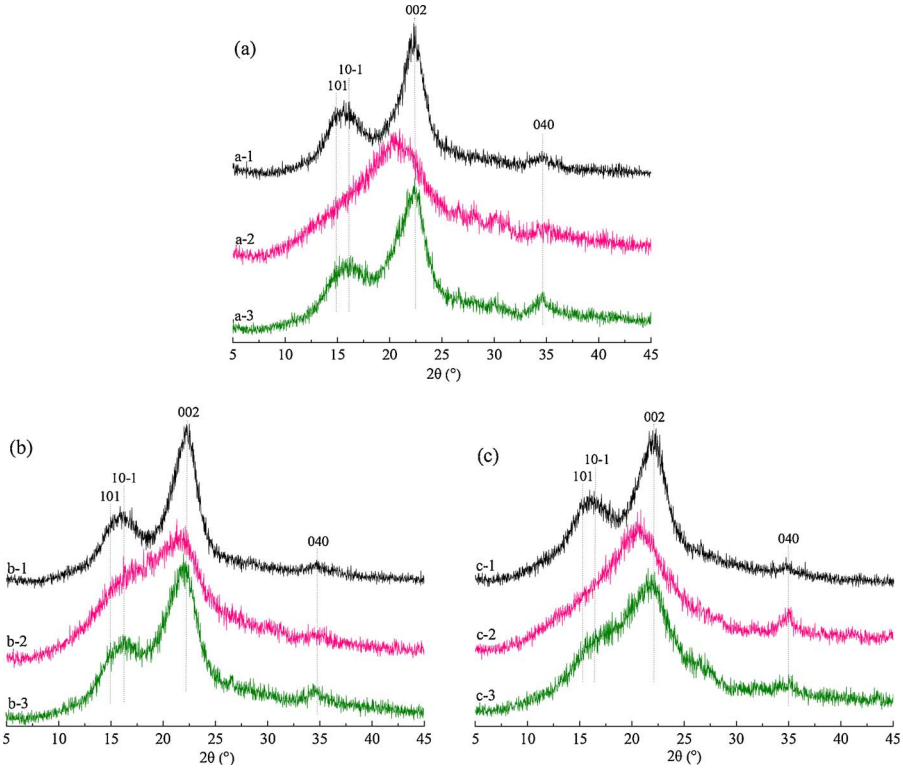

Fig. 6. XRD patterns of different samples: (a) cellulose, (b) holocellulose, (c) SCB, and 1, 2, 3 represent original, MA treated (120 min), MASPR modified (120 min), respectively.

2016GXNSFAA380217), Guangxi Scientific Research and Technological Development Project of China (No. 1598020-1), Guangxi Distinguished Experts Special Foundation of China, and the Scientific Research Foundation of Guangxi University (Grant No. XJPZ160713).

References

Beramendi-Orosco, L. E., Castro-Diaz, M., Snape, C. E., Vane, C. H., & Large, D. J. (2004). Application of catalytic hydropyrolysis for the rapid preparation of lignin concentrates from wood. *Organic Geochemistry, 35*, 61–72.

Boufi, S., & Belgacem, M. N. (2006). Modified cellulose fibres for adsorption of dissolved organic solutes. *Cellulose, 13*, 81–94.

Chen, M., Chen, C., Liu, C., & Sun, R. (2013). Homogeneous modification of sugarcane bagasse with maleic anhydride in 1-butyl-3-methylimidazolium chloride without any catalysts. *Industrial Crops and Products, 46*, 380–385.

Crépy, L., Miri, V., Joly, N., Martin, P., & Lefebvre, J. (2011). Effect of side chain length on structure and thermomechanical properties of fully substituted cellulose fatty esters. *Carbohydrate Polymers, 83*, 1812–1820.

Doczekalska, B., Bartkowiak, M., & Zakrzewski, R. (2014). Esterification of willow wood with cyclic acid anhydrides. *Wood Research, 59*, 85–96.

Fox, S. C., & McDonald, A. G. (2010). Chemical and thermal characterization of three industrial lignins and their corresponding lignin esters. *BioResources, 5*, 990–1009.

Freire, C. S. R., Silvestre, A. J. D., Neto, C. P., Gandini, A., Martin, L., & Mondragon, I. (2008). Composites based on acylated cellulose fibers and low-density polyethylene: Effect of the fiber content, degree of substitution and fatty acid chain length on final properties. *Composites Science and Technology, 68*, 3358–3364.

Gosselink, R., Abacherli, A., Semke, H., Malherbe, R., Kauper, P., Nadif, A., et al. (2004). Analytical protocols for characterisation of sulphur-free lignin. *Industrial Crops and Products, 19*, 271–281.

Gurgel, L. V. A., Júnior, O. K., Gil, R. P. D. F., & Gil, L. F. (2008). Adsorption of Cu(II), Cd (II): And Pb(II) from aqueous single metal solutions by cellulose and mercerized cellulose chemically modified with succinic anhydride. *Bioresource Technology, 99*, 3077–3083.

Hendriks, A. T. W. M., & Zeeman, G. (2009). Pretreatments to enhance the digestibility of lignocellulosic biomass. *Bioresource Technology, 100*, 10–18.

Hundhausen, U., Kloeser, L., & Mai, C. (2015). Usability of maleic anhydride as wood modification agent for the production of medium density fibreboards (MDF). *European Journal of Wood and Wood Products, 73*, 283–288.

Iwamoto, Y., & Itoh, T. (2005). Vapor phase reaction of wood with maleic anhydride (I): Dimensional stability and durability of treated wood. *Journal of Wood Science, 51*, 595–600.

Kai, D., Tan, M. J., Chee, P. L., Chua, Y. K., Yap, Y. L., & Loh, X. J. (2016). Towards lignin-based functional materials in a sustainable world. *Green Chemistry, 18*, 1175–1200.

Kirk, T. K. (1975). Effects of a brown-rot fungus, Lenzites trabea on lignin in spruce wood. *Holzforschung, 29*, 99–107.

Laurichesse, S., & Avérous, L. (2014). Chemical modification of lignins: Towards biobased polymers. *Progress in Polymer Science, 39*, 1266–1290.

Leibbrandt, N. H., Knoetze, J. H., & Görgens, J. F. (2011). Comparing biological and thermochemical processing of sugarcane bagasse: An energy balance perspective. *Biomass and Bioenergy, 35*, 2117–2126.

Liao, Z., Huang, Z., Hu, H., Zhang, Y., & Tan, Y. (2011). Microscopic structure and properties changes of cassava stillage residue pretreated by mechanical activation. *Bioresource Technology, 102*, 7953–7958.

Liu, C., Sun, R., Qin, M., Zhang, A., Ren, J., Xu, F., et al. (2007). Chemical modification of ultrasound-pretreated sugarcane bagasse with maleic anhydride. *Industrial Crops and Products, 26*, 212–219.

Love, G. D., Snape, C. E., & Jarvis, M. C. (1998). Comparison of leaf and stem cell-wall components in barley straw by solid-state ^{13}C NMR. *Phytochemistry, 49*, 1191–1194.

Nakasone, K., Ikematsu, S., & Kobayashi, T. (2016). Biocompatibility evaluation of cellulose hydrogel film regenerated from sugar cane bagasse waste and its in vivo behavior in mice. *Industrial & Engineering Chemistry Research, 55*, 30–37.

Pandey, A., Soccol, C. R., Nigam, P., & Soccol, V. T. (2000). Biotechnological potential of agro-industrial residues: I: Sugarcane bagasse. *Bioresource Technology, 74*, 69–80.

Ren, J. L., Sun, R. C., Liu, C. F., Lin, L., & He, B. H. (2007). Synthesis and characterization of novel cationic SCB hemicelluloses with a low degree of substitution. *Carbohydrate Polymers, 67*, 347–357.

Rowell, R. M., Simonsen, R., Hess, S., Plackett, D. V., Cronshaw, D., & Dunningham, E. (1994). Acetyl distribution in acetylated whole wood and reactivity of isolated wood cell-wall components to acetic anhydride. *Wood and Fiber Science, 26*, 11–18.

Sakdaronnarong, C., Saengsawang, A., Siriyutta, A., Jonglertjunya, W., Nasongkla, N., & Laosiripojana, N. (2016). An integrated system for fractionation and hydrolysis of sugarcane bagasse using heterogeneous catalysts in aqueous biphasic system. *Chemical Engineering Journal, 285*, 144–156.

Sun, R. C., Fang, J. M., Tomkinson, J., Geng, Z. C., & Liu, J. C. (2001). Fractional isolation: physico-chemical characterization and homogeneous esterification of hemicelluloses from fast-growing poplar wood. *Carbohydrate Polymers, 44*, 29–39.

Sun, J. X., Xu, F., Sun, X. F., Xiao, B., & Sun, R. C. (2005). Physico-chemical and thermal characterization of cellulose from barley straw. *Polymer Degradation and Stability, 88*, 521–531.

Sun, J. X., Sun, X. F., Sun, R. C., & Su, Y. Q. (2004). Fractional extraction and structural characterization of sugarcane bagasse hemicelluloses. *Carbohydrate Polymers, 56*, 195–204.

Sun, J. X., Sun, X. F., Zhao, H., & Sun, R. C. (2004). Isolation and characterization of cellulose from sugarcane bagasse. *Polymer Degradation and Stability, 84*, 331–339.

Tang, L., Huang, B., Yang, N., Li, T., Lu, Q., Lin, W., et al. (2013). Organic solvent-free and efficient manufacture of functionalized cellulose nanocrystals via one-pot tandem reactions. *Green Chemistry, 15*, 2369–2373.

Tran, C. D., Chen, J., Keum, J. K., & Naskar, A. K. (2016). A new class of renewable thermoplastics with extraordinary performance from nanostructured lignin-elastomers. *Advanced Functional Materials, 26*, 2677–2685.

Upton, B. M., & Kasko, A. M. (2016). Strategies for the conversion of lignin to high-value polymeric materials: Review and perspective. *Chemical Reviews, 116*, 2275–2306.

Vaidya, A. A., Newman, R. H., Campion, S. H., & Suckling, I. D. (2014). Strength of

adsorption of polyethylene glycol on pretreated Pinus radiata wood and consequences for enzymatic saccharification. *Biomass and Bioenergy, 70*, 339–346.
Vaidya, A. A., Gaugler, M., & Smith, D. A. (2016). Green route to modification of wood waste: Cellulose and hemicellulose using reactive extrusion. *Carbohydrate Polymers, 136*, 1238–1250.
Xiao, B., Sun, X. F., & Sun, R. C. (2001). The chemical modification of lignins with succinic anhydride in aqueous systems. *Polymer Degradation and Stability, 71*, 223–231.
Xu, F., Jiang, J., Sun, R., She, D., Peng, B., Sun, J., et al. (2008). Rapid esterification of wheat straw hemicelluloses induced by microwave irradiation. *Carbohydrate Polymers, 73*, 612–620.
Yang, J., Zhang, X., & Xu, F. (2015). Design of cellulose nanocrystals template-assisted composite hydrogels: insights from static to dynamic alignment. *Macromolecules, 48*, 1231–1239.
Zhang, H., & Wu, S. (2014). Enhanced enzymatic cellulose hydrolysis by subcritical carbon dioxide pretreatment of sugarcane bagasse. *Bioresource Technology, 158*, 161–165.
Zhang, Y., Gan, T., Hu, H., Huang, Z., Huang, A., Zhu, Y., et al. (2014). A green technology for the preparation of high fatty acid starch esters: Solid-phase synthesis of starch laurate assisted by mechanical activation with stirring ball mill as reactor. *Industrial & Engineering Chemistry Research, 53*, 2114–2120.
Zhang, Y., Gan, T., Luo, Y., Zhao, X., Hu, H., Huang, Z., et al. (2014). A green and efficient method for preparing acetylated cassava stillage residue and the production of all-plant fibre composites. *Composites Science and Technology, 102*, 139–144.
Zhao, X., Zhang, Y., Hu, H., Huang, Z., Yang, M., Chen, D., et al. (2016). Effect of mechanical activation on structure changes and reactivity in further chemical modification of lignin. *International Journal of Biological Macromolecules, 91*, 1081–1089.
Zhao, X., Huang, Z., Zhang, Y., Yang, M., Chen, D., Huang, K., et al. (2017). Efficient solid-phase synthesis of acetylated lignin and a comparison of the properties of different modified lignins. *Journal of Applied Polymer Science, 134*, 44276.
Zhou, H., Chang, Y., Wu, X., Yang, D., & Qiu, X. (2015). Horseradish peroxidase modification of sulfomethylated wheat straw alkali lignin to improve its dispersion performance. *ACS Sustainable Chemistry & Engineering, 3*, 518–523.